



Contents lists available at ScienceDirect

Journal of Sound and Vibration

journal homepage: www.elsevier.com/locate/jsvi

On the slow dynamics of near-field acoustically levitated objects under High excitation frequencies

Dotan Ilssar, Izhak Bucher*

Dynamics Laboratory, Faculty of Mechanical Engineering, Technion – Israel Institute of Technology, Haifa 3200003, Israel

ARTICLE INFO

Article history:

Received 23 November 2014
 Received in revised form
 12 April 2015
 Accepted 12 May 2015
 Available online 6 June 2015

Keywords:

Near-field acoustic levitation
 analytical model
 nonlinear acoustics
 Reynolds equation.

ABSTRACT

This paper introduces a simplified analytical model describing the governing dynamics of near-field acoustically levitated objects. The simplification converts the equation of motion coupled with the partial differential equation of a compressible fluid, into a compact, second order ordinary differential equation, where the local stiffness and damping are transparent. The simplified model allows one to more easily analyse and design near-field acoustic levitation based systems, and it also helps to devise closed-loop controller algorithms for such systems. Near-field acoustic levitation employs fast ultrasonic vibrations of a driving surface and exploits the viscosity and the compressibility of a gaseous medium to achieve average, load carrying pressure. It is demonstrated that the slow dynamics dominates the transient behaviour, while the time-scale associated with the fast, ultrasonic excitation has a small presence in the oscillations of the levitated object. Indeed, the present paper formulates the slow dynamics under an ultrasonic excitation without the need to explicitly consider the latter. The simplified model is compared with a numerical scheme based on Reynolds equation and with experiments, both showing reasonably good results.

© 2015 Elsevier Ltd. All rights reserved.

1. Introduction

Near-field acoustic levitation, which is also known as squeeze film levitation, occurs when a planar object is placed in proximity to a vibrating surface. Consequently, a thin layer of the ambient gas, commonly referred to as squeeze film, is trapped in the clearance between the vibrating surface and the adjacent planar object. The abovementioned phenomenon depends on the viscosity of the gas, which plays an important role such that the flow regime can be referred to as viscous (e.g. [1,2]). Thanks to its viscous behaviour, the gas which resides inside the squeeze film cannot be immediately squeezed out. Additionally, due to the compressibility of the entrapped gas, the average pressure inside the film is usually higher than the surroundings, what results in a load carrying force. This force can levitate the planar object above the vibrating surface, assuming the former is freely suspended. One possible application of the near-field acoustic levitation phenomenon is a non-contacting bearing [3] where the stiffness and damping properties are important.

The abovementioned levitation mechanism can be represented by a combination of two distinct forces. The first force considered here is the displacement related levitation force emanating from the compressibility of the gas. Langlois [2] who proposed to use Reynolds equation for the modelling of the squeeze film, employed first order perturbation on this

* Corresponding author. Tel.: 972 77 8873153.

E-mail addresses: dilssar@technion.ac.il (D. Ilssar), bucher@technion.ac.il (I. Bucher).

equation. Nevertheless, this approach cannot predict the nominal value of the levitation force, which is a nonlinear effect. Salbu [4] evaluated the levitation force using a simplified model of the squeeze film based on Boyle's law, under the assumption of mass conservation. This assumption suggests that there is no flow at the peripheries of the film, what violates the boundary conditions since it leads to a discontinuity in the pressure distribution. However, the solution presented by Salbu [4] is suitable at extremely high squeeze numbers (this measure will be introduced below). Minikes *et al.* [5] developed an empirical expression which manages to predict the time averaged levitation force for wide intervals of excitation amplitudes (of the vibrating surface) and squeeze numbers. Minikes also showed that a second order perturbation solution of Reynolds equation can approximate this value, but for a limited range of excitation amplitudes. Nevertheless, according to numerical simulations, this range is sufficiently wide for most purposes of near-field acoustic levitation. Therefore the spirit of this approach is adopted in the current study.

The second force needed to be described within the levitation mechanism is the damping force resulting from the viscosity of the gas. This force was studied extensively in the past (e.g. [6–10]), usually in the context of MEMS devices. In all of these studies the clearance between the bounding surfaces was assumed to be oscillating at small amplitudes, and so the squeeze film was modelled by the linearized Reynolds equation [6]. Moreover, Griffin *et al.* [9] made an additional assumption which claims that the clearance varies slowly compared with the cut-off frequency and is thus confined to slow frequencies. Griffin noted that under this assumption, the estimated damping force can be generalized to the case of large displacements. In the current paper it is shown that a similar approach can be utilized for the calculation of the damping force throughout near-field acoustic levitation. The latter is despite the presence of fast oscillations which originate in the high excitation frequency.

It is important to note that the papers mentioned above deal with each of the forces exerted by the film separately, assessing their steady-state values. The latter is carried out for the case where the mean clearance between the bounding surfaces is pre-determined. However, a simplified analytical model which combines these forces in order to describe the time varying dynamics of an acoustically levitated object was not presented in previous publications. Obviously, in this case, the nominal clearance is determined due to equilibrium of forces.

For the purpose of controlling the dynamics of an acoustically levitated object, be it open or closed loop, a manageable mathematical model is essential. Clearly, a full CFD or even a Reynolds equation based model coupled to the structural dynamics, are by far too complex and impractical for devising a control strategy or for assessing the stiffness and damping during design cycles. Indeed, the present paper seeks a simplified analytical model that describes merely the slow evolution of the levitated object, given the enforced rapid oscillations.

The current paper begins with presentation of the governing equations describing the levitation mechanism. Next, based on former numerical schemes (e.g. [11]), it is shown that the dynamics of the levitated object can be represented as a superposition of slow and fast processes. This implies that it is possible to formulate a simplified analytical model which describes merely the slow evolution of the levitated object, given the enforced and nonlinearly coupled fast oscillations. Therefore, such simplified model is developed following two main steps. The first step relates only to the levitation force and results in an equation which represents the slow evolution of the levitated object in absence of damping. Obviously, the second step relates to the damping force and results in modification of the conservative equation so it includes the effect of dissipation. The entire development is carried out under the assumption that the vibrating surface oscillates uniformly – as a rigid piston.

Finally, after a satisfactory numerical verification, an experimental validation of the simplified model is carried out. The results of this validation shows reasonable agreement of both the momentary frequency of the slow oscillations, and the steady state levitation height. However, it is shown in the experiments that there is a significant deviation in the prediction of the damping. Therefore, based on numerous experiments, a linear correction coefficient is determined for the dissipative term in the abovementioned simplified model. That so this model will suit the system on which the experiments were carried out.

2. Problem description

A simplified model of an acoustically levitated object is illustrated in Fig. 1. This model consists of an oscillating surface producing the required excitation, and a freely suspended planar object, which are both cylindrical (disks) and with equal diameters. As can be seen from Fig. 1, in this model, the excitation surface does not deform and it oscillates at a constant

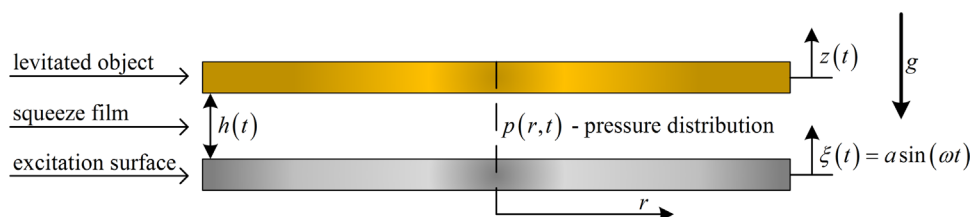


Fig. 1. Schematic layout of the system.

frequency and displacement amplitude. Additionally, the levitated object is subjected only to the gravity and to the pressure acting by the surrounding fluid.

2.1. Formulation of the governing equations

In order to describe the dynamics of the abovementioned system, two equations which couple the film's behaviour with the dynamics of the levitated object, are introduced. The behaviour of the squeeze film is approximated by Reynolds equation which under the assumptions of isothermal conditions, and no lateral angular or tangential motion of the bounding surfaces, takes the following form [2]:

$$\frac{\partial}{\partial r} \left(r h^3 p \frac{\partial p}{\partial r} \right) = 12 \mu r \frac{\partial (p h)}{\partial t} \quad (1)$$

where h is the time dependent air-gap between the levitated object and the excitation surface, p is the pressure distribution inside the squeeze film, r is the radial coordinate, t denotes the time and μ which is taken here as $1.8253 \cdot 10^{-5}$ Pa · sec, stands for the dynamic viscosity of the fluid.

Reynolds equation (1) can be derived from the Navier-Stokes momentum equation and from the continuity equation, under commonly employed assumptions [1]. It is worth mentioning one important assumption concerning the air-gap which is assumed to be much smaller compared with the other dimensions of the system. Accordingly, the normal components of the pressure gradient and the flow velocity are negligible, while the velocity gradients in the transverse directions are negligible as well. As a result, order of magnitude analysis with typical values leaves Reynolds equation merely with viscous and pressure terms.

It was previously mentioned that Reynolds equation cannot describe the overall dynamics of the system, which also depends on the levitated object. Therefore (1) must be coupled with the equation of motion accounting for the dynamics of the levitated object. This equation considers the body force, the pressure distribution inside the squeeze film and the ambient pressure, and so it takes the following form:

$$m \frac{d^2 z}{dt^2} = \int_0^{2\pi} \int_0^{r_0} r (p - p_a) dr d\theta - mg = 2\pi \int_0^{r_0} r (p - p_a) dr - mg. \quad (2)$$

Here, z is the height of the levitated object, which is measured from the nominal position of the excitation surface, m is the mass of the levitated object, r_0 denotes the radii of the bounding surfaces, p_a that is taken here as 101325 Pa, is the ambient pressure and g which is taken as 9.81 m/sec^2 stands for the acceleration due to the gravity.

As mentioned, the excitation surface oscillates uniformly at a constant frequency according to:

$$\xi(t) = a \sin(\omega t) \quad (3)$$

where a , ω are the excitation amplitude and the excitation frequency respectively.

Therefore, the relation between the air-gap h and the levitation height z is:

$$h(t) = z(t) - \xi(t) = z(t) - a \sin(\omega t). \quad (4)$$

Substitution of (4) into (2) yields the equation of motion in terms of the pressure distribution and the air-gap, as (1):

$$m \frac{d^2 h}{dt^2} = 2\pi \int_0^{r_0} r (p - p_a) dr - mg + m \omega^2 a \sin(\omega t). \quad (5)$$

Finally, because the system is axisymmetric, there is no pressure gradient at the centre of the film. Additionally, the pressure at the peripheries of the film is assumed to be equal to the ambient pressure, since the radius of the levitated object is equal to the radius of the excitation surface. The latter is based on Minikes *et al.* [12] which examined this boundary condition using a CFD analysis. Therefore, the boundary conditions of the pressure distribution inside the squeeze film are taken as followings:

$$\left. \frac{\partial p(r, t)}{\partial r} \right|_{r=0} = 0, \quad p(r = r_0, t) = p_a. \quad (6)$$

Thus (1),(5),(6) are used in order to formulate the dynamics of the system illustrated in Fig. 1.

2.2. Preliminary numerical simulations – slow and fast dynamics

As shown by Minikes *et al.* [11], by discretization of the spatial (radial) coordinate to a finite number of nodes, Reynolds equation (1) can be transformed into a set of ODEs as following:

$$\left(\frac{\partial p}{\partial t} \right)_n = \frac{h^2}{12 \mu r_n} \left[p_n \left(\frac{\partial p}{\partial r} \right)_n + r_n \left(\frac{\partial p}{\partial r} \right)_n^2 + r_n p_n \left(\frac{\partial^2 p}{\partial r^2} \right)_n \right] - \frac{p_n}{h} \frac{dh}{dt} \quad (7)$$

where n denotes the index of the radial node.

These equations are solved in time together with the equation of motion (2) or (5), using numerical integration. Here, the spatial derivatives of the pressure distribution in every node are calculated using central differences formulas, while the needed values at the external nodes $n = 1, N$ are calculated according to the boundary conditions (6). By these means, the results illustrated in Fig. 4 (solid black lines), were produced.

From this figure and from previous experiments and simulations (e.g. [11,13]) it is clear that the dynamic response of an acoustically levitated object is composed of two distinct time scales. The first time scale relates to the slow transient oscillations which are typically 2–3 orders of magnitude slower than the excitation frequency. The second time scale is associated with the fast oscillations whose basic frequency equals to the excitation frequency. These low-amplitude fast oscillations do not disappear at steady state. Consequently, and according to (4), the air-gap between the levitated object and the excitation surface takes the following general form:

$$h(t) = \bar{h}(t) + \chi(t) - a \sin(\omega t) \tag{8}$$

where χ represents the fast oscillations of the levitated object, and \bar{h} stands for the slow evolution of the air-gap, or equivalently the slow evolution of the levitated object.

It is the main goal of this paper to formulate a simplified equation from which \bar{h} can be found without having to solve (7).

Denoting the initial air-gap h_0 , the following non-dimensional measures are defined:

$$P = \frac{p}{p_a}, \quad H = \frac{h}{h_0}, \quad \bar{H} = \frac{\bar{h}}{h_0}, \quad R = \frac{r}{r_0}, \quad T = \omega t, \quad \sigma = \frac{12\mu\omega r_0^2}{p_a \bar{h}^2} = \frac{12\mu\omega r_0^2}{p_a h_0^2 \bar{H}^2}, \quad \varepsilon = \frac{a}{\bar{h}} = \frac{a}{h_0 \bar{H}} \tag{9}$$

Two important measures are σ , representing the squeeze number and ε which is the small non-dimensional excitation amplitude. Indeed, σ , ε are the prevailing factors, whose magnitudes control the momentary behaviour of the system, as will be shown below.

Substituting (9) into (1),(5),(6) yields the non-dimensional Reynolds equation:

$$\frac{\partial}{\partial R} \left(RH^3 P \frac{\partial P}{\partial R} \right) = \sigma \bar{H}^2 R \frac{\partial (PH)}{\partial T} \tag{10}$$

alongside the non-dimensional equation of motion:

$$\frac{d^2 H}{dT^2} = \frac{2\pi p_a r_0^2}{m h_0 \omega^2} \int_0^1 R(P-1) dR - \frac{g}{h_0 \omega^2} + \varepsilon \bar{H} \sin(T) \tag{11}$$

and the non-dimensional boundary conditions:

$$\left. \frac{\partial P(R, T)}{\partial R} \right|_{R=0} = 0, \quad P(R=1, T) = 1. \tag{12}$$

3. Development of the simplified analytical model

In order to develop a simplified analytical model describing the slow dynamics of an acoustically levitated object, two main steps are followed. In the first step, the pressure rise due to the rapid enforced oscillations is computed, leading to the instantaneous time averaged levitation force, with which the gap-dependent stiffness of the film can be found. Next, the damping force which dissipates energy and depends on the rate of the slowly varying gap is found. These two steps yield a single ordinary differential equation describing the slow dynamics of the system illustrated in Fig. 1.

3.1. Formulation of the undamped system's equation of motion

The initial step considers the degenerated system shown in Fig. 2. Here, since the upper object is fixed, the nominal air-gap \bar{h} is constant. The outcome of this step is the averaged force exerted on the fixed object due to the pressure elevation which is caused due to the compressibility of the gas. This force will then be used in order to describe the instantaneous averaged levitation force acting on a freely suspended object.

According to Fig. 2 and the relations (9), the non-dimensional air-gap varies as following:

$$H = \bar{H}[1 - \varepsilon \sin(T)]. \tag{13}$$

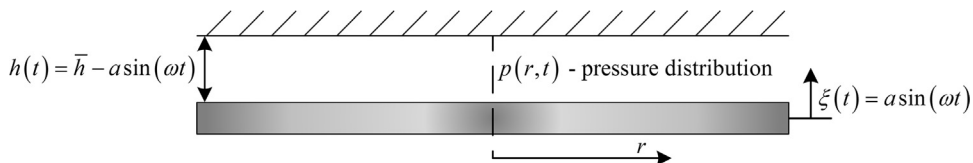


Fig. 2. Schematic layout of the degenerated system in which the upper object is fixed.

It was already mentioned that nonlinear effects should be taken into account when the time averaged force or pressure are to be found. Therefore, the non-dimensional pressure distribution is represented as a second order asymptotic series, as suggested by Minikes *et al.* [5]:

$$P(R, T) = 1 + \epsilon \Pi_A(R, T) + \epsilon^2 \Pi_B(R, T) + \mathcal{O}(\epsilon^3) \tag{14}$$

while as aforesaid, ϵ functions as a small parameter.

Substitution of (13) and (14) into the non-dimensional Reynolds equation (10) provides the following two leading orders coupled equations:

$$\mathcal{O}(\epsilon): \frac{\partial}{\partial R} \left(R \frac{\partial \Pi_A}{\partial R} \right) = R \sigma \left(\frac{\partial \Pi_A}{\partial T} - \cos(T) \right) \tag{15}$$

$$\mathcal{O}(\epsilon^2): R \sigma \frac{\partial(\Pi_A \sin(T))}{\partial T} + (\Pi_A - 3 \sin(T)) \frac{\partial}{\partial R} \left(R \frac{\partial \Pi_A}{\partial R} \right) + \frac{\partial}{\partial R} \left(R \frac{\partial \Pi_B}{\partial R} \right) + R \left(\frac{\partial \Pi_A}{\partial R} \right)^2 = R \sigma \frac{\partial \Pi_B}{\partial T}. \tag{16}$$

In order to balance the leading order equation (15), the following general solution is suggested for Π_A :

$$\Pi_A(R, T) = \Pi_1(R) \cos(T) + \Pi_2(R) \sin(T). \tag{17}$$

By substituting (17) into (15) and performing harmonic balance, two ODEs are produced. Solving these equations such that Π_1, Π_2 vanish at the peripheries in order to satisfy the boundary conditions (12), leads to the following solutions:

$$\begin{aligned} \Pi_1(R) &= \frac{\text{ber}_0(\sqrt{\sigma}R)\text{bei}_0(\sqrt{\sigma}) - \text{bei}_0(\sqrt{\sigma}R)\text{ber}_0(\sqrt{\sigma})}{\text{ber}_0^2(\sqrt{\sigma}) + \text{bei}_0^2(\sqrt{\sigma})} \\ \Pi_2(R) &= 1 - \frac{\text{ber}_0(\sqrt{\sigma}R)\text{ber}_0(\sqrt{\sigma}) + \text{bei}_0(\sqrt{\sigma}R)\text{bei}_0(\sqrt{\sigma})}{\text{ber}_0^2(\sqrt{\sigma}) + \text{bei}_0^2(\sqrt{\sigma})} \end{aligned} \tag{18}$$

where $\text{ber}_\nu(R), \text{bei}_\nu(R)$ are ν^{th} order Kelvin functions of the first kind.

One can notice that substitution of (17) into the second order equation (16) gives rise to terms dependent on second temporal harmonics, and also to time independent terms. Therefore, in order to balance (16), the following general solution is suggested for Π_B :

$$\Pi_B(R, T) = \Pi_3(R) \cos(2T) + \Pi_4(R) \sin(2T) + \Pi_5(R). \tag{19}$$

Substitution of (17) and (19) into (16) and averaging over one excitation period, generates the following equation:

$$(\Pi_2 - 3) \frac{d}{dR} \left(R \frac{d\Pi_2}{dR} \right) + 2 \frac{d}{dR} \left(R \frac{d\Pi_5}{dR} \right) + \Pi_1 \frac{d}{dR} \left(R \frac{d\Pi_1}{dR} \right) + R \left[\left(\frac{d\Pi_1}{dR} \right)^2 + \left(\frac{d\Pi_2}{dR} \right)^2 \right] = 0. \tag{20}$$

Since Π_1, Π_2 are known, (20) is a linear inhomogeneous ODE for Π_5 . The solution of this equation, under the boundary conditions (12) (Π_5 vanishes at the peripheries), yields the time independent part of the gauge pressure distribution:

$$\Pi_5(R) = \frac{1}{4} \left[5 - \frac{\text{ber}_0^2(\sqrt{\sigma}R) + \text{bei}_0^2(\sqrt{\sigma}R) + 4 [\text{ber}_0(\sqrt{\sigma}R)\text{ber}_0(\sqrt{\sigma}) + \text{bei}_0(\sqrt{\sigma}R)\text{bei}_0(\sqrt{\sigma})]}{\text{ber}_0^2(\sqrt{\sigma}) + \text{bei}_0^2(\sqrt{\sigma})} \right]. \tag{21}$$

At this point the time averaged levitation force is calculated by integration on the total pressure (inside and outside the film) over the area of the upper object, and averaging over one excitation period:

$$F_{levitation} = \frac{1}{2\pi} \int_0^{2\pi} \int_0^{2\pi} \int_0^1 R(P - 1) dR d\theta dT = 2\pi \epsilon^2 \int_0^1 R \Pi_5(R) dR = \pi \epsilon^2 K(\sigma) \tag{22}$$

where $F_{levitation}$ has been normalized by $p_a r_0^2$.

Here $K(\sigma)$ quantifies the force level as a function of the squeeze number and it attains the following closed form:

$$K(\sigma) = \frac{5}{4} \left[1 + \sqrt{\frac{2}{\sigma}} \cdot \frac{\text{bei}_0(\sqrt{\sigma}) [\text{ber}_1(\sqrt{\sigma}) + \text{bei}_1(\sqrt{\sigma})] + \text{ber}_0(\sqrt{\sigma}) [\text{ber}_1(\sqrt{\sigma}) - \text{bei}_1(\sqrt{\sigma})]}{\text{ber}_0^2(\sqrt{\sigma}) + \text{bei}_0^2(\sqrt{\sigma})} \right]. \tag{23}$$

Fig. 3, which describes the functions $\Pi_5(R), K(\sigma)$, shows a very good correlation to the results that were presented by Minikes *et al.* [5] who made a similar analysis for a long rectangular system. Examination of Fig. 3, shows that beyond $\sigma \approx 50$, the averaged levitation force does not increase considerably with the increment of the squeeze number. Hence for the purpose of effective levitation vs. power usage, it is sufficient to choose excitation frequencies and amplitudes which lead to such squeeze numbers.

Finally, it is important to mention that the levitation force emanates from the pressure profile built by the rapid oscillations of the system, due to the compressibility of the gas. Therefore, since the evolution of the levitated object is much slower than the excitation (see Fig. 4), its contribution to the averaged levitation force can be neglected. Moreover, it was shown in the past (e.g. [11]) that the amplitude of the levitated object's fast oscillations is 2–3 orders of magnitude smaller than the excitation amplitude and so the contribution of these oscillations can be neglected as well. Consequentially, the overall dynamics of the levitated object can be neglected when calculating $F_{levitation}$, which means that (22)-(23) provide a

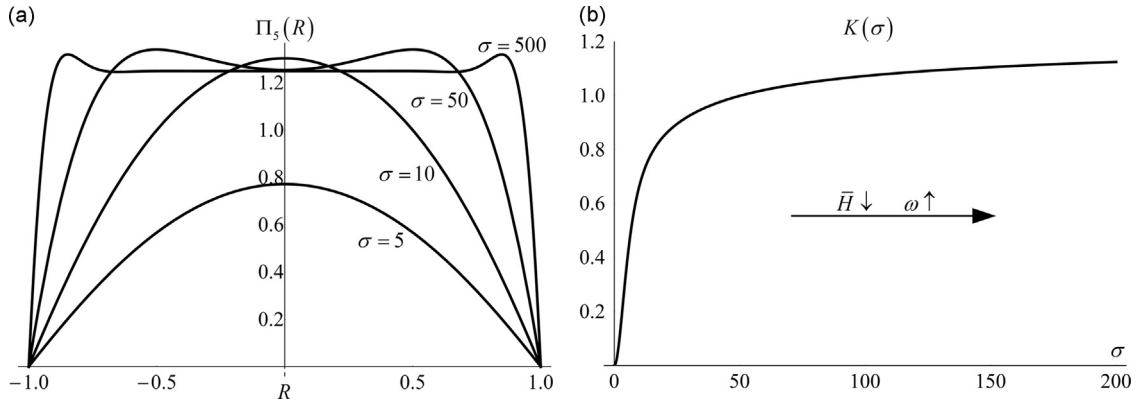


Fig. 3. (a) The time independent part of the gauge pressure distribution $\Pi_5(R)$ Vs. the spatial coordinate for various squeeze numbers, (b) The function $K(\sigma)$ Vs. the squeeze number.

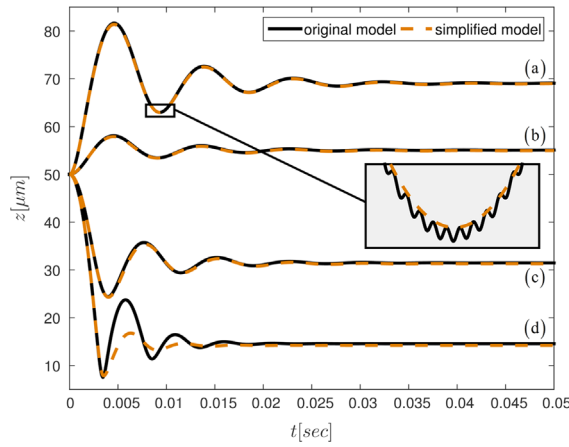


Fig. 4. Comparison between dynamic responses (whose parameters appear in Table 1 and Table 2), obtained from the original model and from the simplified model.

good approximation for the slowly varying levitation force acting on a freely suspended object. Therefore, the equation of motion describing the slow dynamics of the original system (Fig. 1) in absence of damping, can be formulated. This is done by averaging the equation of motion (11) over one excitation period and substituting the averaged levitation force (22):

$$\frac{d^2\bar{H}}{dT^2} = \frac{\pi r_0^2 p_a a^2 K(\sigma(\bar{H}))}{m\omega^2 h_0^3 \bar{H}^2} - \frac{g}{\omega^2 h_0}. \tag{24}$$

Obviously, here the levitated object is no longer taken as fixed and therefore K is a functional of σ which depends on the slow evolution \bar{H} .

3.2. Adding the effect of energy loss and damping

It is well known that the viscosity plays an important role in the phenomenon of near-field acoustic levitation [1,2]. Thus it is clear that equation (24) needs to be supplemented by a term representing energy dissipation. This is done considering only the contribution of the slow evolution, while the damping forces acting due to the rapid oscillations are omitted since they affect merely the fast oscillations of the levitated object and the lost power at these frequencies is fed back by the forced excitation.

For sake of calculating the damping force acting due to the slow evolution, small oscillations around a given nominal air-gap $h_l = h_0 H_l$, are considered. Consequently, small pressure variations around the averaged pressure distribution are considered as well. Therefore, after averaging out the fast terms, the non-dimensional air-gap and pressure distribution take the following forms:

$$\bar{H}(T) = H_l + \varepsilon_l^\beta \Delta H(T), \quad \bar{P}(R, T) = 1 + \varepsilon_l^2 \Pi_5(\sigma_l, R) + \varepsilon_l^\beta \Delta P(R, T) \tag{25}$$

where $\varepsilon_l = \varepsilon(\bar{H} = H_l) = \varepsilon \bar{H} / H_l$, $\sigma_l = \sigma(\bar{H} = H_l) = \sigma \bar{H}^2 / H_l^2$.

Substitution of (25) into the non-dimensional Reynolds equation (10) yields the following equation:

$$\begin{aligned} & \frac{\partial}{\partial R} \left(R(H_I + \varepsilon_I^\beta \Delta H)^3 (1 + \varepsilon_I^2 \Pi_5 + \varepsilon_I^\beta \Delta P) \frac{\partial (\varepsilon_I^2 \Pi_5 + \varepsilon_I^\beta \Delta P)}{\partial R} \right) \\ & = \varepsilon_I^\beta \sigma \bar{H}^2 R \frac{\partial (\Delta H + \varepsilon_I^2 \Pi_5 \Delta H + H_I \Delta P + \varepsilon_I^\beta \Delta H \Delta P)}{\partial T}. \end{aligned} \tag{26}$$

It can be seen that this equation can be balanced only if $0 \leq \beta \leq 2$, while in order to strengthen the small displacements assumption, and in order not to obviate the contribution of Π_5 , $\beta = 2$ is substituted into (26). After neglecting high order terms, this equation yields the following modified form of the linearized Reynolds equation for compressible gas [6]:

$$\mathcal{O}(\varepsilon_I^2): \frac{\partial}{\partial R} \left(R \frac{\partial (\Pi_5 + \Delta P)}{\partial R} \right) = \sigma_I R \left(\frac{1}{H_I} \frac{d\Delta H}{dT} + \frac{\partial \Delta P}{\partial T} \right). \tag{27}$$

In order to solve (27), the following boundary and initial conditions are suggested:

$$|\Delta P(R, T)| < \infty, \quad \Delta P(R = 1, T) = 0, \quad \Delta H(T = 0) = 0, \quad \Delta P(R, T = 0) = 0. \tag{28}$$

The boundary conditions claim that the pressure variation is finite and that it equals to zero at the film’s edge, in order to satisfy the boundary conditions (12). In addition, the initial conditions were chosen arbitrarily at the nominal state.

Due to the linearity of the problem, separation of variables is suggested:

$$\Delta P(R, T) = \gamma(R)\Gamma(T) \tag{29}$$

Substituting (29) into the homogenous equation that corresponds to (27), and solving the Sturm-Liouville problem obtained using (28), provides the following eigenvalues and eigenfunctions:

$$\alpha_n = j_{0,n}^2, \quad \gamma_n(R) = J_0(j_{0,n}R), \quad n = 1, 2, 3, \dots \tag{30}$$

here $j_{0,n}$ stands for the n^{th} zero of $J_0(R)$ which is the zeroth order Bessel function of the first kind.

Development of (27) in a generalized Fourier series using these eigenfunctions, transforms it into the following form:

$$\sum_{n=1}^{\infty} R J_0(j_{0,n}R) \left[\frac{d\Gamma_n}{dT} + \frac{j_{0,n}^2 (A_n + \Gamma_n)}{\sigma_I} + \frac{2}{H_I j_{0,n} J_1(j_{0,n})} \frac{d\Delta H}{dT} \right] = 0 \tag{31}$$

where A_n denote the constant generalized Fourier coefficients of Π_5 , and Γ_n are the time dependent generalized Fourier coefficients of the pressure variation function ΔP .

Comparison of coefficients provides a single temporal ODE that depends on both Γ_n and ΔH . In order to relate these functions so that an expression for the pressure variation function could be easily found for any given change in the air-gap, Laplace transform is applied to this ODE. After imposing initial conditions, the abovementioned Laplace transform yields the following expression, while $\tilde{\bullet}$ stands for the Laplace transform of \bullet , and s is the Laplace variable:

$$\tilde{\Gamma}_n(s) = - \left(s + \frac{j_{0,n}^2}{\sigma_I} \right)^{-1} \left(\frac{2s\Delta\tilde{H}}{H_I j_{0,n} J_1(j_{0,n})} + \frac{j_{0,n}^2 A_n}{\sigma_I s} \right). \tag{32}$$

Based on former experiments and numerical simulations (e.g. [11, 13]), very low evolution frequencies are considered. Thus, $s \rightarrow i\Omega$, $\Omega \ll \Omega_c$ is substituted into (32), as suggested by Griffin *et al.* [9], while Ω is the evolution frequency normalized by the excitation frequency ω , and $\Omega_c = j_{0,1}^2/\sigma_I$ is an approximated value of the non-dimensional cut-off frequency in which the magnitudes of the spring and damping forces exerted by the film, are equal [8]. According to Blech [8] one can obtain Griffin’s results by adding to the linearized Reynolds equation the assumption of incompressibility where $\sigma \rightarrow 0$. Clearly, this approach is not valid here since $\sigma \gg 1$, and so the spirit of Griffin’s approach should be employed. Therefore, considering frequencies below cut-off, one obtains:

$$\tilde{\Gamma}_n(i\Omega) = - \left(i\Omega + \frac{j_{0,n}^2}{\sigma_I} \right)^{-1} \left(\frac{2i\Omega\Delta\tilde{H}}{H_I j_{0,n} J_1(j_{0,n}R)} + \frac{j_{0,n}^2 A_n}{\sigma_I i\Omega} \right) \approx - \left(\frac{2\sigma_I}{H_I j_{0,n}^3 J_1(j_{0,n})} i\Omega\Delta\tilde{H} + \frac{A_n}{i\Omega} \right). \tag{33}$$

Substituting the inverse transform of (33) into (29) provides the complete expression of the pressure variation function, in time:

$$\Delta P(R, T) = \sum_{n=1}^{\infty} \gamma_n(R)\Gamma_n(T) = - \underbrace{\sum_{n=1}^{\infty} \frac{2\sigma_I J_0(j_{0,n}R)}{H_I j_{0,n}^3 J_1(j_{0,n})} \frac{d\Delta H}{dT}}_{\Delta P_1(R,T)} - \underbrace{\sum_{n=1}^{\infty} A_n J_0(j_{0,n}R)}_{\Pi_5(R)}. \tag{34}$$

Finally, the damping force acting due to the slow evolution is calculated by integration on the total averaged pressure (inside and outside the film), over the area of the levitated object. Here, due to the linearity of the problem, the contribution of the

averaged levitation force vanishes, thus:

$$F_{damping} = \int_0^{2\pi} \int_0^1 R(\bar{P}-1) dR d\theta = -2\pi\epsilon_1^2 \int_0^1 R\Delta P_1(R, T) dR = -\frac{\pi\sigma_1\epsilon_1^2}{8H_1} \frac{d\Delta H}{dT} = -\frac{3\pi\mu\omega r_0^2 a^2}{2p_a h_0^4 H_1^5} \frac{d\Delta H}{dT} \tag{35}$$

where $F_{damping}$ has been normalized by $p_a r_0^2$.

Evidentially the damping force related to slow motion (35), depends on the rate of the slowly changing averaged air-gap. It was mentioned above that the dominant frequency of the original system's slow oscillations is much lower than the cut-off frequency, as has been verified numerically and experimentally for a wide range of parameters. Consequently, and according to Griffin *et al.* [9], H_1 can be referred to as the quasi-static part of \bar{H} that varies in large amplitudes, while ΔH is the variable part of \bar{H} which as aforesaid changes much slower than the cut-off frequency. Therefore, and according to (25), the following approximations can be used:

$$H_1 \approx \bar{H}, \quad \frac{d\Delta H}{dT} \approx \frac{1}{\epsilon_1^2} \frac{d\bar{H}}{dT} \approx \frac{1}{\epsilon^2} \frac{d\bar{H}}{dT} \tag{36}$$

Supplementing the conservative equation of motion (24) with the damping force (35) under the assumptions (36), yields the averaged equation of motion of the damped system:

$$\frac{d^2\bar{H}}{dT^2} = \frac{C_s K(\sigma(\bar{H}))}{\bar{H}^2} - \frac{C_d}{\bar{H}^3} \frac{d\bar{H}}{dT} - G \tag{37}$$

where the non-dimensional constants C_s, C_d, G are the followings:

$$C_s = \frac{\pi r_0^2 p_a a^2}{m \omega^2 h_0^3}, \quad C_d = \frac{3\pi \mu r_0^4}{2m \omega h_0^3}, \quad G = \frac{g}{\omega^2 h_0} \tag{38}$$

Eqs. (37), (38) represent the slow dynamics of an acoustically levitated object under the enforced fast oscillations indicated by (3). The former is a nonlinear ordinary differential equation in terms of the slow evolution of the levitated object, which is a function of the initial conditions and the fast driving excitation.

It is important to note that since we wish to examine large displacements of the levitated object, no local approximation methods are implemented on (37) in the scope of this paper. I.e. all of the results shown in the following sections were obtained by solving (37) numerically. Clearly, (37) can be solved for the steady-state levitation height by nulling all the derivatives with respect to time. This would yield a transcendental equation that has to be solved numerically.

3.3. Numerical verification

It should be reminded that both steps of the development are based on the assumption that the non-dimensional excitation amplitude ϵ is small. Therefore, as ϵ grows, all the asymptotic assumptions weaken and the accuracy of the simplified model (37) deteriorates.

In order to evaluate the influence of the non-dimensional excitation amplitude, on the accuracy of (37), comparison to the original model (10)-(12) seems appropriate. Indeed, Fig. 4 presents the dynamic responses of several different masses levitated by the system whose parameters are specified in Table 1, as obtained numerically from the simplified model and from the original model. Additionally, Table 2 summarises a few important characteristics of the responses appear in Fig. 4. This table presents the maximal and the steady state non-dimensional excitation amplitude of each response and it also shows the maximal and the steady state relative errors between the results.

The results presented in Fig. 4 and Table 2 show a very good correlation between the simplified model and the original model. While clearly, since the simplified model considers merely the slow evolution of the levitated object, the results obtained using this model don't describe its fast oscillations which exist in the results obtained using the original model. However, it can be seen that as the air-gap decreases, the accuracy of (37) deteriorates, as the non-dimensional excitation amplitude increases. Further investigation shows that if the non-dimensional excitation amplitude stays below $\epsilon \approx 0.3$ throughout the dynamic response, the errors between the models are negligible at steady state and also during the transient response.

The whole development carried out above, was executed under the assumption that both the excitation amplitude and the excitation frequency stay constant. However, one can notice that this development also holds when the excitation

Table 1
The physical parameters under which the simulations in Fig. 4 and Fig. 5 were carried out.

Radii of the excitation surface and the levitated object	10 mm
Excitation amplitude (nominal value in Fig. 5)	5 μm
Excitation frequency	28.5 kHz

Table 2
Important characteristics of the dynamic responses presented in Fig. 4.

Curve	Mass [g]	ϵ_{ss}	ϵ_{max}	Steady state error	Maximal error
a	10	0.0725	0.1	0.1245%	0.3147%
b	20	0.0910	0.1	0.1842%	0.3469%
c	80	0.1596	0.2058	0.5232%	1.8782%
d	450	0.3516	0.6367	2.5224%	35.4566%

amplitude varies slowly such that:

$$\frac{d\epsilon}{dT} \ll \epsilon^2. \quad (39)$$

It can be seen from Table 2 that a typical value of the non-dimensional excitation amplitude is of order $\mathcal{O}(10^{-1})$. Therefore, the condition (39) usually holds if the excitation amplitude varies more than one order of magnitude slower than the excitation frequency. Fortunately, since the frequency of the slow oscillations complies with this criterion, such low frequencies are sufficient for controlling the slow dynamics of the levitated object. And therefore the simplified model (37) seems suitable for the considered applications.

Fig. 5 presents three dynamic responses which their parameters are specified in Table 1 and Table 3, as obtained from the simplified model and from the original model (after adding necessary terms that consider the variation of the amplitude). From this figure it is clear that the good correlation between the results is kept under time variant excitation amplitude, assuming the abovementioned conditions are met.

4. Experimental validation

Validation of the simplified model developed in the previous section was carried out using the experimental setup presented in Fig. 6. In this setup, the required excitation is provided by a driving levitation device that consists of two main components. The first component is an off-shelf piezoelectric (Langevin) actuator that is designated to operate at ~ 28.5 kHz, in which it resonates at its first elastic longitudinal mode. The second component is an aluminium stepped horn which produces mechanical amplification of the excitation amplitudes generated by the Langevin actuator. For sake of efficiency, the horn was designed to resonate at its first elastic longitudinal mode, at the same frequency as the actuator. At this designated frequency the horn magnifies the displacement at its base by 1:4.41.

Experiments show that while working in the vicinity of the designated frequency, the deformation of the excitation surface is small. In the frequency range under which the experiments were carried out, the maximal deflection of this surface was less than 8% of its piston-like displacement. Therefore, the configuration presented in Fig. 6 seems suitable for verification of the theoretical model, which was derived under the assumption that the excitation surface vibrates uniformly.

The abovementioned device was driven by a high voltage amplifier fed by a signal generator that allows controlling both the amplitude and the frequency of the excitation. This device was used in order to levitate two different masses weighing 2.7 g and 7.91 g, while in order to satisfy the boundary conditions (12), the radii of these masses were chosen to be equal to the radius of the excitation surface (10 mm).

Numerous experiments, in which the abovementioned round objects (masses) were levitated, under various constant excitation amplitudes and frequencies, were carried out. During these experiments, the dynamic responses of the masses were measured using a laser interferometer. Fig. 7 displays two representative examples, while the parameters under which they were executed, are presented in Table 4. Fig. 7 also presents the corresponding responses obtained from the simplified model (37) using the same parameters.

It is important to note that in each of the experiments, the non-dimensional excitation amplitude ϵ stayed below 0.15 throughout the dynamic response. Therefore, the corresponding responses obtained from (37) represent accurately the exact solutions of Eqs. (10)–(12). And so, the comparison between the experimental results and the results obtained from (37) is used in order to estimate the accuracy of the original Reynolds equation based physical model.

Fig. 8 presents the relative error between the steady-state levitation heights obtained from the experiments and from the simplified model, as function of the steady-state height obtained experimentally. Here, the relative error was calculated according to:

$$\text{relative error} = \frac{\bar{z}_{ss, \text{experiment}} - \bar{z}_{ss, \text{simulation}}}{\bar{z}_{ss, \text{experiment}}} \cdot 100\%. \quad (40)$$

From Fig. 8 it can be seen that the steady-state errors are very low. Additionally, one can notice a trend according to which the error grows with the steady-state levitation height. While at low levitation heights, the model overestimates the real steady-state height, and at significant heights it underestimates it. This trend is consistent with the results presented by Wang *et al.* [13] which compared experimental steady-state levitation heights, to the values obtained by solving (10)–(12) numerically.

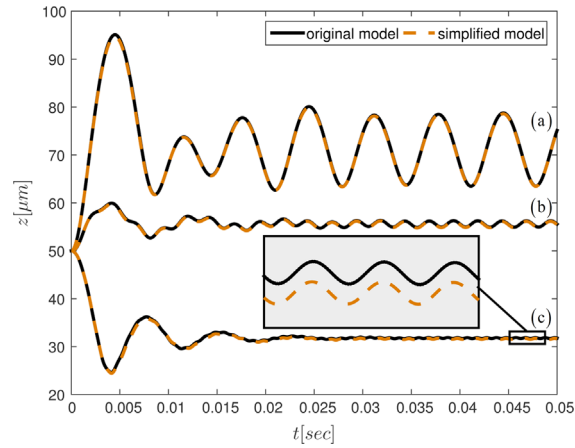


Fig. 5. Comparison between dynamic responses (whose parameters appear in Table 1 and Table 3), obtained from the original model and from the simplified model, under time variant excitation amplitudes.

Table 3
Supplementary parameters of the simulations appear in Fig. 5.

Curve	Mass [g]	Excitation amplitude [μm]
a	10	$5 + \sin(150t)$
b	20	$5 + \sin(400t)$
c	80	$5 + \sin(1000t)$

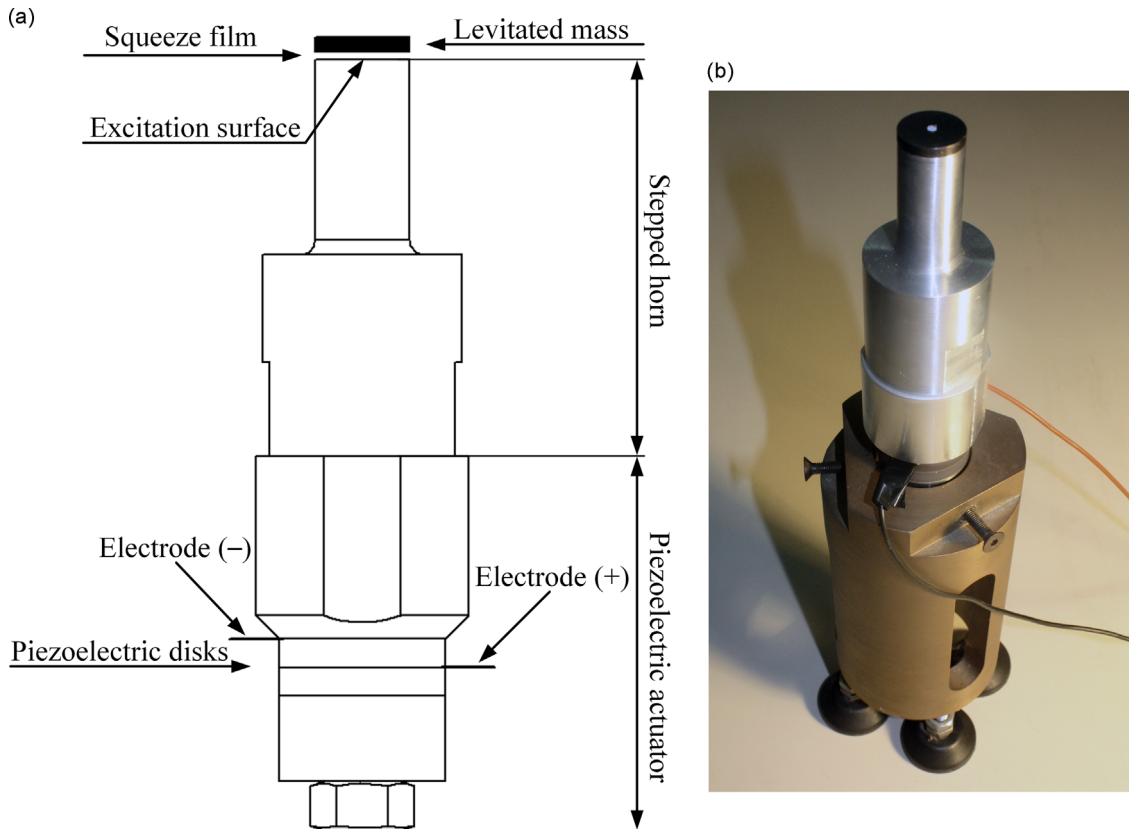


Fig. 6. Schematic layout and photograph of the experimental setup.

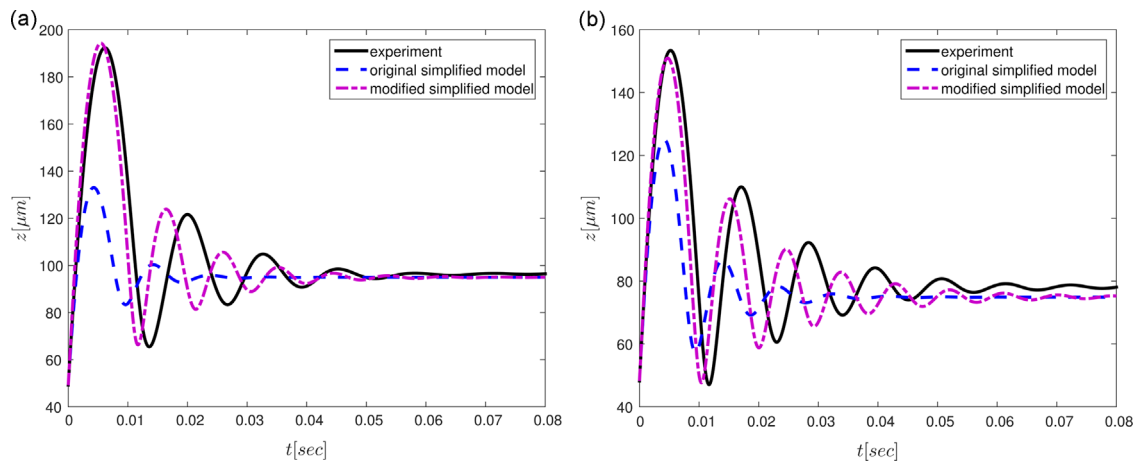


Fig. 7. Two representative dynamic responses (whose parameters appear in Table 4), obtained experimentally and theoretically using the simplified model (before and after modification).

Table 4

The parameters under which the experiments and the simulations in Fig. 7 and Fig. 9 were carried out.

Example	Mass [g]	Excitation frequency [Hz]	Excitation amplitude [μm]
a	2.7	28,350	4.93
b	7.91	28,350	5.16

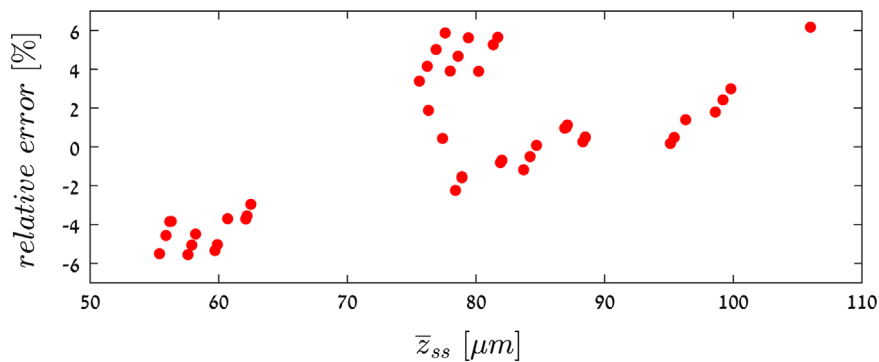


Fig. 8. The relative error between the steady-state levitation heights obtained from the experiments and from the simplified model Vs. the steady-state height obtained experimentally.

Contrary to the very good agreement between experimental and the theoretical steady-state values, one can notice a significant overestimation of the damping, which can be explained by two main reasons. The first reason is the fact that in practice, in addition to its desired vertical motion, the levitated mass also undergoes lateral oscillations that cannot be fully suppressed. These oscillations occur when the centre of the levitated mass is slightly displaced from the centre of the excitation surface [14]. Additionally, due to the break of symmetry, the lateral oscillations give rise to an additional tilting motion. The unwanted lateral and tilting motions result in energy leakage from the levitation mechanism, and therefore they affect its behaviour.

The second reason responsible for the significant damping overestimation originate in the fact that Reynolds equation refer to the flow inside the film as pure viscous. However, turbulence caused by the fast oscillations can weaken this assumption and change the behaviour of the film [1].

In order to modify (37), so it will describe the behaviour of the system presented in Fig. 6 more accurately, a corrected expression for damping coefficient C_d was sought – denoted as C'_d . For this sake, first, the corrected value that suits each of the experiments was found by minimizing the norm between the envelope of each experimental response and the envelope of its corresponding theoretical response. These envelopes were represented by fifth order polynomials found using linear least squares on the local maximums of the responses. The corrected states of the representative examples shown in Fig. 7, in which the values of C'_d are optimal, are presented in Fig. 9 along their envelopes. For comparison, this figure also presents the corresponding experimental results alongside their envelopes.

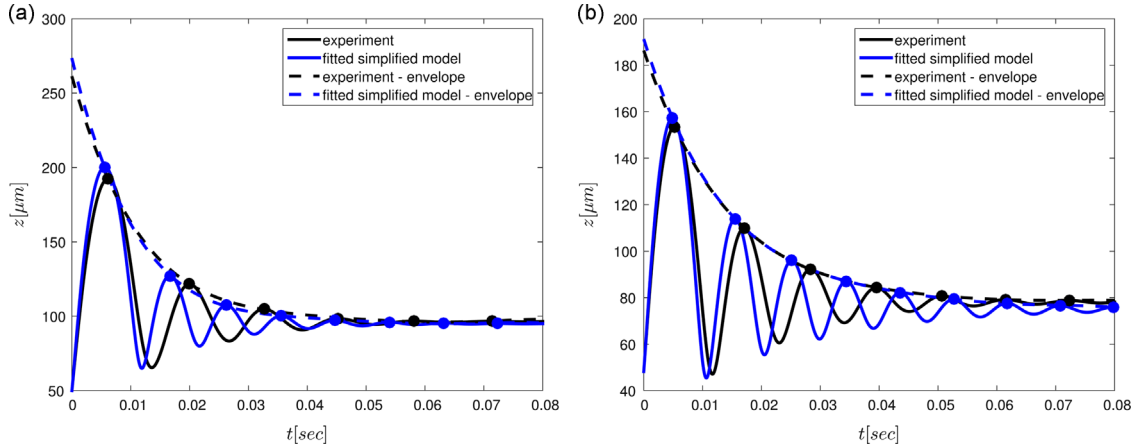


Fig. 9. Calculation of the corrected damping coefficients for the two representative examples (whose parameters appear in Table 4), using envelope curve-fitting.

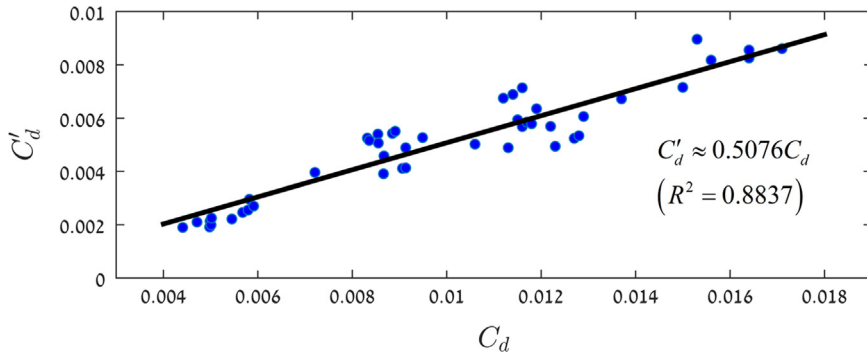


Fig. 10. Finding the relation between the original and the corrected damping coefficients, using linear fitting.

Fig. 10 presents the corrected damping coefficients obtained by implementing the abovementioned procedure on each of the experiments, against their original values. From this figure it can be seen that the relation between the corrected and the original damping coefficients can be approximated by a linear slope as following:

$$C'_d \approx 0.5076C_d. \tag{41}$$

In addition to the experimental and the theoretical responses displayed in Fig. 7, this figure also presents the corresponding responses obtained from (37) by using the corrected damping coefficients calculated according to (41). From this figure it can be seen that the modification of the model improved the agreement with the experimental results significantly. However, one can notice a moderate error estimating the frequency of the oscillations. This error is approximated between 10% – 30% and can be related to the same reasons that cause the damping overestimation.

5. Conclusions

It was shown that the dynamics of an acoustically levitated object can be represented as a superposition of slow and fast processes. For applications of controlling the levitated object’s dynamics, the slow process is usually more important. Hence, a simplified analytical model which describes merely the slow evolution of the levitated object was developed, following two main steps. The first step of the development addresses merely to the conservative forces, and the second step relates solely to the dissipative forces.

The second step of the development, in which the dissipative forces are calculated, considers only the slow evolution of the system and ignores the fast oscillations of both the levitated object and the excitation surface. The latter implies that the excitation form (i.e. the spatial deformation of the excitation surface), hardly affects the dissipative forces related to the slow dynamics of the system.

Numerical validation of the simplified model developed in this paper was carried by comparison to the original, well-known Reynolds equation based model. The comparison was carried out for the case where the excitation amplitude is constant, and also for the case in which it varies relatively slowly in time. The good agreement of the latter suggests that the simplified model can be used for applications of controlling the slow dynamics of an acoustically levitated object.

Finally, an experimental validation of the simplified model was carried out, while due to the good agreement achieved in the numerical verification, this validation was referred to as an examination of the original Reynolds equation based model. It was shown that the theoretical models provide a reasonably good prediction of both the momentary frequency of the slow oscillations, and the steady state levitation height. However, a significant, yet consistent, error was obtained in the prediction of the damping force. Therefore, a single linear correction coefficient was determined for the dissipative term in the abovementioned simplified model, what adjusted it to suit the system on which the experiments were performed. From the good agreement between the experiments and the results obtained using the modified model, it is implied that the simplified model developed in this paper can be adjusted empirically. That in order to describe other setups which complies with the assumptions presented in [sections 2, 3](#).

Finally, it is the authors' opinion that despite the deviation of the experiments from the theoretical results, the Reynolds equation based model and its simplification presented in this paper are useable for design and for assessing the dynamical performance of acoustically levitated objects.

Acknowledgements

This research was funded by the Israeli Ministry of science, Technology and Space.

The second author would like to acknowledge the support of the ISF grant 030072 that generated the foundations and funding for earlier results leading to this work.

References

- [1] W.A. Gross, L. Matsch, V. Castelli, A. Eshel, J. Vohr, M. Wildmann, *Fluid film lubrication*, John Wiley and Sons, Inc, New York, NY, 1980.
- [2] W. Langlois, *Isothermal squeeze films*, DTIC Document, 1961.
- [3] S. Zhao, S. Mojrzisch, J. Wallaschek, An ultrasonic levitation journal bearing able to control spindle center position, *Mechanical Systems and Signal Processing* 36 (2013) 168–181.
- [4] E. Salbu, Compressible squeeze films and squeeze bearings, *Journal of Basic Engineering* 86 (1964) 355–364.
- [5] A. Minikes, I. Bucher, S. Haber, Levitation force induced by pressure radiation in gas squeeze films, *The Journal of the Acoustical Society of America* 116 (2004) 217–226.
- [6] M. Bao, H. Yang, Squeeze film air damping in MEMS, *Sensors and Actuators A: Physical* 136 (2007) 3–27.
- [7] M.-H. Bao, *Micro mechanical transducers: pressure sensors, accelerometers and gyroscopes*, Elsevier, 2000.
- [8] J. Blech, On isothermal squeeze films, *Journal of Lubrication Technology* 105 (1983) 615–620.
- [9] W.S. Griffin, H.H. Richardson, S. Yamanami, A study of fluid squeeze-film damping, *Journal of Basic Engineering* 88 (1966) 451–456.
- [10] A. Minikes, I. Bucher, G. Avivi, Damping of a micro-resonator torsion mirror in rarefied gas ambient, *Journal of Micromechanics and Microengineering* 15 (2005) 1762.
- [11] A. Minikes, I. Bucher, Coupled dynamics of a squeeze-film levitated mass and a vibrating piezoelectric disc: numerical analysis and experimental study, *Journal of sound and vibration* 263 (2003) 241–268.
- [12] A. Minikes, I. Bucher, Comparing numerical and analytical solutions for squeeze-film levitation force, *Journal of fluids and structures* 22 (2006) 713–719.
- [13] Y. Wang, B. Wei, Mixed-Modal Disk Gas Squeeze Film Theoretical and Experimental Analysis, *International Journal of Modern Physics B* 27 (2013).
- [14] E. Matsuo, Y. Koike, K. Nakamura, S. Ueha, Y. Hashimoto, Holding characteristics of planar objects suspended by near-field acoustic levitation, *Ultrasonics* 38 (2000) 60–63.